

Evidence of a bactericidal permeability increasing protein in an invertebrate, the *Crassostrea gigas* Cg-BPI

Marcelo Gonzalez*, Yannick Gueguen*, Delphine Destoumieux-Garzón*, Bernard Romestand*, Julie Fievet*, Martine Pugnière†, Françoise Roquet†, Jean-Michel Escoubas**‡, Franck Vandenbulcke§, Ofer Levy¶, Laure Sauné*, Philippe Bulet||, and Evelyne Bachère*•**

*Ifremer, Centre National de la Recherche Scientifique, Université Montpellier 2, Unité Mixte de Recherche 5119, Ecosystèmes Lagunaires, Place E. Bataillon, CC80, 34095 Montpellier Cedex 5, France; †Centre National de la Recherche Scientifique, Unité Mixte de Recherche 5236, Centre d'Études d'Agents Pathogènes et Biotechnologie pour la Santé, Institut de Biologie, 34965 Montpellier, France; §Ecologie Numérique et Ecotoxicologie, Université des Sciences et Technologies de Lille, 59655 Villeneuve d'Ascq, France; ¶Children's Hospital Boston and Harvard Medical School, Boston, MA 02115; and ||Atheris Laboratories, CP314, 1233 Bernex-Geneva, Switzerland

Edited by Jerrold P. Weiss, University of Iowa, Coralville, IA, and accepted by the Editorial Board September 20, 2007 (received for review March 14, 2007)

A cDNA sequence with homologies to members of the LPS-binding protein and bactericidal/permeability-increasing protein (BPI) family was identified in the oyster *Crassostrea gigas*. The recombinant protein was found to bind LPS, to display bactericidal activity against *Escherichia coli*, and to increase the permeability of the bacterial cytoplasmic membrane. This indicated that it is a BPI rather than an LPS-binding protein. By *in situ* hybridization, the expression of the *C. gigas* BPI (*Cg-bpi*) was found to be induced in hemocytes after oyster bacterial challenge and to be constitutive in various epithelia of unchallenged oysters. Thus, *Cg-bpi* transcripts were detected in the epithelial cells of tissues/organs in contact with the external environment (mantle, gills, digestive tract, digestive gland diverticula, and gonad follicles). Therefore, Cg-BPI, whose expression profile and biological properties are reminiscent of mammalian BPIs, may provide a first line of defense against potential bacterial invasion. To our knowledge, this is the first characterization of a BPI in an invertebrate.

antimicrobial | epithelia | hemocyte | mollusk | oyster innate immunity

Marine invertebrates including bivalve mollusks have evolved in the continuous presence of microorganisms. The oysters, such as *Crassostrea gigas*, harbor a diverse microflora both on their surface (epibiosis) and inside the body cavities and hemolymph (endobiosis). They have developed an efficient immune system for maintaining balance with commensal and pathogenic bacteria, in particular with the Gram-negative *Vibrio* spp. abundant in their tissues/organs. LPS from Gram-negative bacteria play an important role in the interaction and activation of the innate immune system including the antimicrobial defense (1, 2). In invertebrates, LPS-binding proteins (LBP) participate in the transduction of cellular signals from LPS. LBPs have been characterized in the freshwater crayfish *Pacifastacus leniusculus* (3), the shrimp *Litopenaeus stylirostris* (4), the earthworm *Eisenia foetida* (5), and the silkworm *Bombyx mori* (6). In mammals, LBP is an acute phase plasma protein constitutively secreted by liver that induces cellular responses (7). In particular, LBP participates in the acute mobilization of circulating neutrophils to sites of tissue injury. Stored in the mobilized neutrophils, antimicrobial peptides and the bactericidal/permeability-increasing protein (BPI) contribute to the elimination of bacteria (8, 9). BPI, another LBP, is a 55-kDa cationic protein specifically active against Gram-negative bacteria. It increases the permeability of the bacterial membranes (10). Accumulated extracellularly, BPI opsonizes bacteria, which enhances phagocytosis by neutrophils (11). LBP and BPI are structurally related, with 45% sequence identity. They have a coordinated function in the response to invading bacteria. The antibacterial BPI displays LPS-neutralizing properties and suppresses LPS inflammatory activity whereas LBP is an acute-phase reactant (8, 12) that displays a concentration-dependent modulation of LPS activity. At low

(basal) concentrations, LBP enhances LPS signaling by increasing LPS delivery to monocytes and other responsive cells, whereas at high concentration it inhibits the endotoxic activity of LPS by facilitating its delivery to plasma lipoproteins, thereby detoxifying it (13). With genomic and transcriptomic approaches, LBP/BPI-related genes have been identified in nonmammalian vertebrates and in invertebrates. These include the carp *Cyprinus carpio* (14), the rainbow trout *Onchorhynchus mykiss* (15), the Atlantic cod *Gadus morhua* (16), the nematode *Caenorhabditis elegans* (17), and recently the mollusk *Biomphalaria glabrata* (18). This suggests a conservation of this LPS-mediated immune reaction. However, because the functional properties of these proteins have not been characterized, they could not be classified either as a LBP or a BPI.

Screening of the *C. gigas* hemocyte EST library (www.ifremer.fr/GigasBase) (19) led to the identification of a sequence with homologies with mammalian LBP/BPIs. To discriminate between LBP and BPI, the full-length cDNA was cloned and the recombinant protein was produced in *Pichia pastoris*. We showed that it displays LPS-binding and bactericidal activities and that it increases cytoplasmic membrane permeability of *Escherichia coli*. Interestingly, Cg-BPI resembled human BPI (hBPI) not only by its structural and biological properties, but also by the localization of gene expression and its expression profile in response to bacterial challenge. Altogether, these results indicate that the gene identified in oyster encodes a BPI-related protein, Cg-BPI.

Results

Identification of an Oyster cDNA Encoding a LBP/BPI Protein. A 596-bp cDNA sequence (GenBank accession no. BQ427321) was identified in the oyster hemocyte EST library previously published (19). The deduced 128-aa sequence was homologous to the C-terminal domain of mammalian LBP/BPI proteins. The full-length cDNA sequence (GenBank accession no. AY165040) was obtained by screening the 36,864 clones from the *C. gigas* hemocyte cDNA

Author contributions: Y.G., D.D.-G., and E.B. designed research; M.G., Y.G., D.D.-G., B.R., J.F., M.P., F.R., J.-M.E., F.V., L.S., and P.B. performed research; M.P., F.R., and F.V. contributed new reagents/analytic tools; M.G., D.D.-G., B.R., M.P., F.R., J.-M.E., F.V., O.L., P.B., and E.B. analyzed data; and M.G., Y.G., D.D.-G., P.B., and E.B. wrote the paper.

The authors declare no conflict of interest.

This article is a PNAS Direct Submission. J.P.W. is a guest editor invited by the Editorial Board.

Abbreviations: LBP, LPS-binding protein; BPI, bactericidal/permeability-increasing protein; ONPG, O-nitrophenyl- β -D-galactopyranoside; hBPI, human BPI; rhBPI, recombinant hBPI; hLBP, human LBP; AU, arbitrary unit.

*Present address: Institut National de la Recherche Agronomique, Université de Montpellier 2, Unité Mixte de Recherche 1133, Ecologie Microbienne des Insectes et Interactions Hôte-Pathogène, Place E. Bataillon, CC54, 34095 Montpellier Cedex 5, France.

**To whom correspondence should be addressed. E-mail: evelyne.bachere@ifremer.fr.

© 2007 by The National Academy of Sciences of the USA

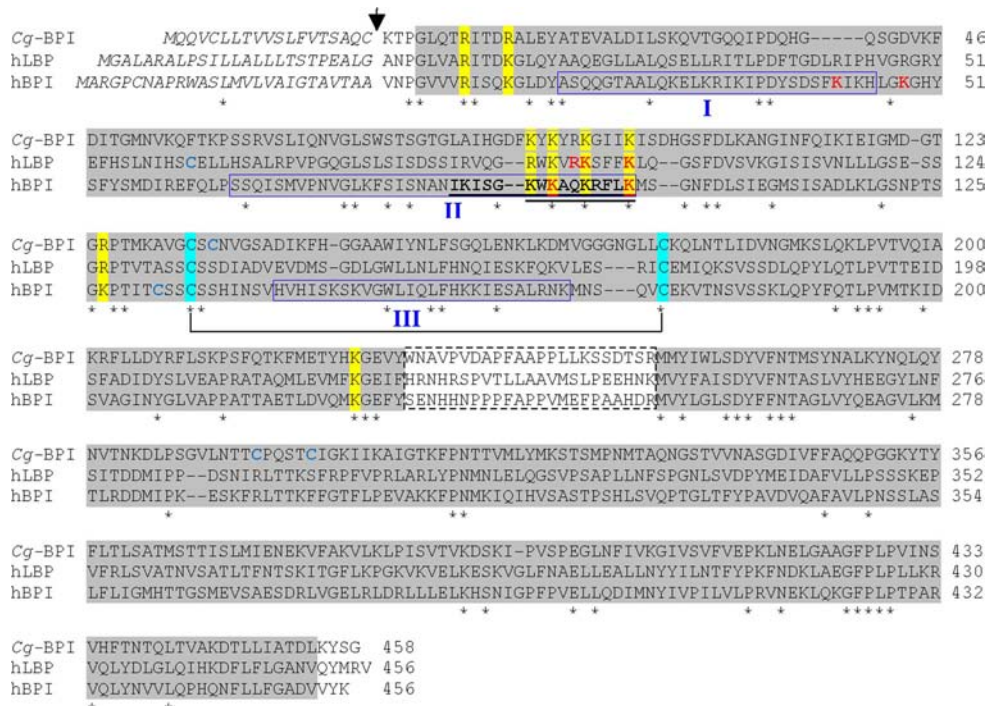


Fig. 1. Sequence homology of *Cg-BPI* with hLBP and hBPI. The amino acid sequences of *Cg-BPI*, hLBP, and hBPI precursor proteins have been deduced from the cDNA clones with GenBank accession nos. AY165040, M35533, and J04739, respectively. Alignment was performed with ClustalW. Conserved residues are indicated by asterisks. Amino acid numbers refer to the mature proteins. An arrow indicates the putative cleavage site by the signal peptidase. The N- and C-terminal barrel-type domains characterized for hBPI as well as the corresponding sequences in hLBP and *Cg-BPI* are highlighted in gray. The proline-rich central domain is boxed with a dashed line. The three functional regions of hBPI, which display LPS-binding activity, are boxed in blue and labeled I, II, and III. Synthetic peptides from hBPI displaying both antibacterial and LPS-binding activities are underlined. Conserved positions of lysines/arginines are highlighted in yellow. Residues required (hLBP) or supposed to be required (hBPI) for LPS binding are shown in red. The four lysines (K in the one-letter code) shown in red in hBPI are conserved residues involved in interaction with LPS (46). Conserved cysteines (C in the one-letter code) forming the single disulfide bond in hBPI are highlighted in blue. Extra cysteines are in blue.

library using the 596-bp cDNA as a probe. It was found to consist in a 1,784-bp ORF with a single typical polyadenylation signal (AATAAAA) between nucleotides 1,675 and 1,681 in the 3' UTR. The deduced 477-aa sequence starts with a predicted 19-aa hydrophobic signal peptide (Fig. 1). The 458-aa putative mature protein displays a calculated molecular mass of 50.1 kDa. Alignment with human LBP (hLBP) (SwissProt accession no. P18428; 46% similarity) and BPI (SwissProt accession no. P17213; 44% similarity) as well as structure modeling showed that the oyster protein has the two conserved domains characteristic of LBP/BPI proteins (Fig. 1). As in mammalian LBP/BPIs, the N-terminal domain displays three cysteines, two of which (at positions 133 and 175) correspond to the conserved disulfide bond (Fig. 1). Two additional cysteines occur at positions 294 and 299 in the C-terminal domain. The putative mature protein is cationic with a calculated pI of 9.3. It contains a high number of lysines (21 over 226 residues in the N-terminal domain), three of which are conserved in hLBP and hBPI (Fig. 1). The construction of an unrooted phylogenetic tree showed that the oyster LBP/BPI clusters with the ascidian *Ciona intestinalis* LBP/BPI (SwissProt accession no. AK115574, 46% similarity) and that they form a group with fish LBP/BPIs and avian BPI, as well as with mammalian BPIs and LBPs (data not shown).

Recombinant Protein Production and Structural Characterization. The protein encoded by the full-length cDNA (GenBank accession no. AY165040) was produced in the recombinant system of *P. pastoris* and purified from culture supernatants. Analyzed by SDS/PAGE, the protein preparation displayed one single band with an apparent molecular mass of 60 kDa (Fig. 2). The identity of the protein was further established by a combination of peptide mass fingerprint

and tandem MS analyses. Thus, 56 peaks between *m/z* 772.495 and *m/z* 3,206.702 were unambiguously identified as tryptic fragments of the recombinant protein (data not shown). The sequence coverage of the matched protein was 70% overlapping with the amino acid sequence deduced from the cDNA.

LPS-Binding, Antibacterial, and Membrane-Permeabilizing Activities. The recombinant protein was shown to bind LPS (Fig. 3) as well as its hydrophobic lipid component, lipid A (data not shown), using plasmon surface resonance. The apparent *K*_D values for LPS binding were measured at 3.1×10^{-8} M assuming that LPS molecules were in a monomeric state (see *Materials and Methods*).

Because both BPI and LBP bind LPS but differ in that BPI additionally displays antibacterial and membrane-disrupting properties, we further investigated the last two mechanisms. Antibacterial activity was assayed against the short-chain LPS *E. coli* SBS363 and the smooth *E. coli* ML35 (Table 1). The recombinant protein demonstrated antibacterial activity against *E. coli* SBS363 with a minimal inhibitory concentration value of 0.3 μ M identical to that obtained with recombinant hBPI (rhBPI₂₁). However, it was not active against the *E. coli* ML35 up to 10 μ M. Against *E. coli* SBS363, full bactericidal activity was observed after 3 h in the presence of 1 μ M r*Cg*-BPI versus 0.25 μ M for rhBPI₂₁ (Fig. 4A). In addition, the oyster recombinant protein disrupted the bacterial cytoplasmic membrane. This was evidenced by treating the lactose permease-deficient *E. coli* ML35 with 5 and 10 μ M of the protein and simultaneously monitoring the hydrolysis of *O*-nitrophenyl- β -D-galactopyranoside (ONPG), used as a substrate for the cytoplasmic β -galactosidase. Like rhBPI₂₁, the oyster recombinant protein

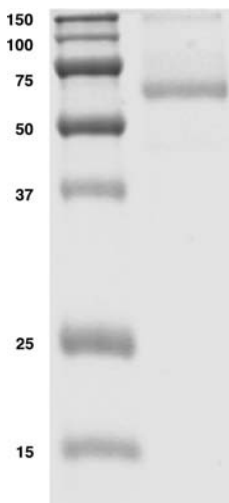


Fig. 2. rCg-BPI visualized by SDS/PAGE. rCg-BPI ($0.5 \mu\text{g}$) was loaded onto 12% SDS/PAGE and stained with Coomassie blue. The molecular mass markers are presented on the left (numbers are in kilodaltons).

induced a significant dose-dependent ONPG hydrolysis 11 min after protein addition versus 5 min for rhBPI₂₁ (Fig. 4B). Because the protein identified in *C. gigas* combines LPS-binding activity with bactericidal and membrane-permeabilizing properties, we conclude that it is a BPI-related protein further named *Cg*-BPI.

***Cg*-bpi Gene Expression Is Constitutive in Oyster Epithelia and Induced in Hemocytes After Bacterial Challenge.** The length of the *Cg*-bpi mRNA was estimated at 2 kb by Northern blot analysis of oyster hemocyte total RNA. One single reactive band was detected on the blot (data not shown).

The time course of *Cg*-bpi gene expression was analyzed in response to bacterial challenge using quantitative *in situ* hybridization with ^{35}S -radiolabeled riboprobes. This methodology gives access to the amounts of transcript of interest [quantified as arbitrary units (AU)] in individual cells and to the percentage of cells expressing that transcript. In circulating hemocytes from unchallenged oysters, the abundance of the *Cg*-bpi transcripts was measured at 10.38 ± 2.2 AU (Fig. 5A). However, it increased significantly 15 h after challenge (45.2 ± 15.2 AU; $P < 0.05$) with a peak at 24 h (128.8 ± 16.7 AU; $P < 0.05$). The transcript abundance decreased at 48 h (49.8 ± 14.9 AU; $P < 0.05$) down to

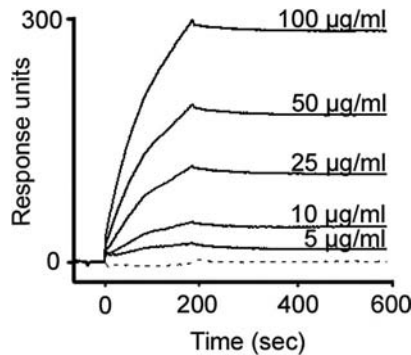


Fig. 3. rCg-BPI binds to LPS. Surface plasmon resonance analysis of rCg-BPI-lipid interactions. The sensorgrams depict the interactions of LPS with rCg-BPI (black lines) or recombinant gp120 used as an irrelevant protein (dashed line) immobilized onto a CM5 chip. LPS and lipid A were injected at a flow rate of $50 \mu\text{l}/\text{min}$. The control sensorgrams (with immobilized protein) were subtracted from the measuring sensorgrams illustrated.

Table 1. Antibacterial activity of rCg-BPI and rhBPI₂₁ against *E. coli* strains with long- or short-chain LPS

Strain	LPS	Minimal inhibitory concentration,* μM	
		rCg-BPI	rhBPI ₂₁
<i>E. coli</i> SBS363	Short-chain	0.3	0.3
<i>E. coli</i> ML35	Long-chain	>10	5

*Determined in poor broth medium.

values observed at 15 h (Fig. 5A). Remarkably, concomitant with the increase in *Cg*-bpi transcript abundance in hemocytes, the percentage of *Cg*-bpi-expressing cells increased in circulating hemocytes. Indeed, whereas in unchallenged oysters $\approx 22\%$ of circulating hemocytes expressed *Cg*-bpi transcripts, they were 30% at 15 h and up to 70% at 24 h after bacterial challenge. At 48 h, the percentage of hemocytes expressing *Cg*-bpi was similar to that observed in unchallenged oysters (Fig. 5A).

In parallel, *Cg*-bpi expression was analyzed by *in situ* hybridization

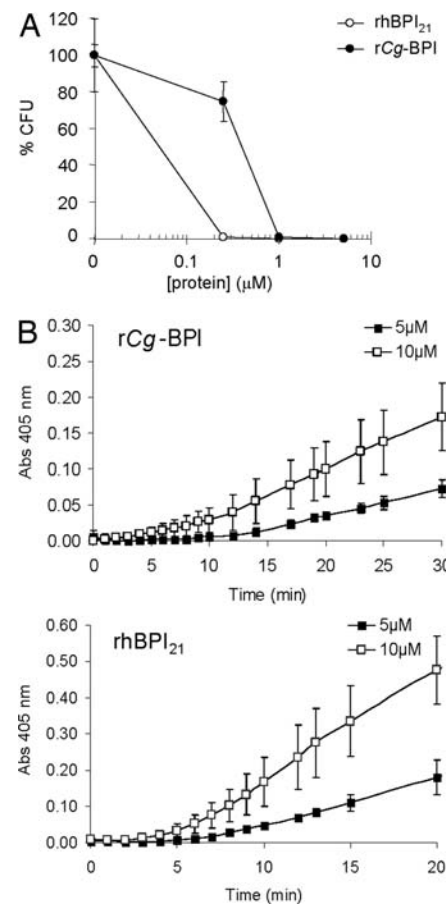


Fig. 4. rCg-BPI displays both bactericidal and membrane-permeabilizing properties. (A) Bactericidal activity of rCg-BPI. *E. coli* SBS363 (5×10^4 cfu/ml) were incubated for 3 h with 0.25 , 1 , and $5 \mu\text{M}$ rCg-BPI (filled circles) or rhBPI₂₁ (open circles) in 10 mM sodium phosphate (pH 7.4) containing 200 mM NaCl. Viability is expressed as a percentage of control cfu \pm SEM. (B) Effect of rCg-BPI on *E. coli* cytoplasmic membrane. *E. coli* ML35 was exposed to rCg-BPI or rhBPI₂₁ at $5 \mu\text{M}$ (filled squares) and $10 \mu\text{M}$ (open squares) or an equal volume of protein buffer in the presence of 2.5 mM ONPG. Substrate hydrolysis indicative of cytoplasmic membrane permeabilization was monitored at 405 nm . In all experiments, the OD measured in the controls (protein buffer) was subtracted from that measured in the presence of rCg-BPI or rhBPI. Data are representative of three independent experiments. Error bars indicate SEM.

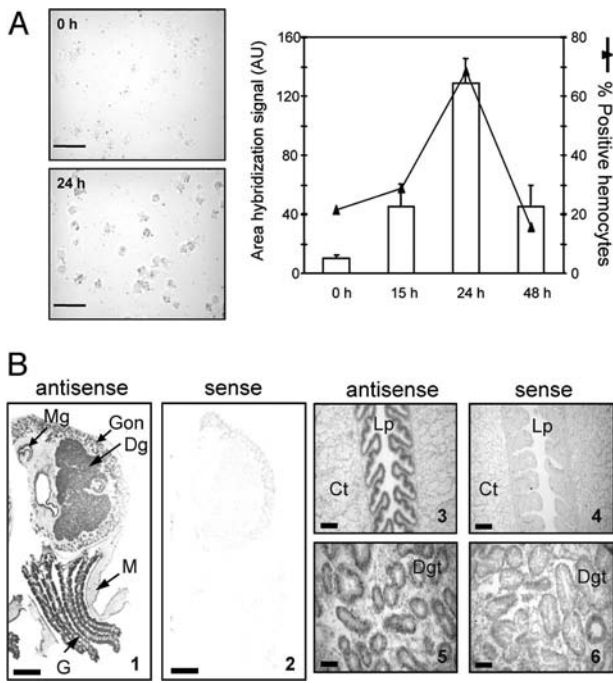


Fig. 5. *Cg-bpi* gene expression analysis. (A) *Cg-bpi* gene expression is induced in hemocytes of oysters subjected to a bacterial challenge. Hemocytes were collected 0, 15, 24, and 48 h after challenge, and *Cg-bpi* transcripts were quantified by [³⁵S] *in situ* hybridization. Silver grains resulting from the contact of [³⁵S] emission with autoradiographic emulsion were counted over the time course in cytocentrifuged hemocytes. Photographs show the silver grains in hemocytes collected from oysters before (0 h) and 24 h after microbial challenge (24 h). (Scale bars: 50 μ m.) For quantification, 100 hemocytes were analyzed at every time point. Histograms show the signals obtained in individual hemocytes after quantification with ImageJ software (National Center for Biotechnology Information). Data are expressed as AU corresponding to area pixels of silver grains within hemocytes. Data represent mean values \pm SD. The percentage of circulating hemocytes expressing *Cg-bpi* transcripts over the time course is shown with diamonds (solid line). (B) *Cg-bpi* gene expression occurs in epithelia of unchallenged oysters. Tangential sections of *C. gigas* were analyzed by [³⁵S] *in situ* hybridization using a *Cg-bpi* antisense riboprobe (*B1*, *B3*, and *B5*) as well as a sense riboprobe (controls, *B2*, *B4*, and *B6*). Labeling appeared in most tissues. The highest hybridization signals were observed in epithelia from gills (G), mantle (M), digestive glands (Dg), gonads (Gon), and midgut epithelia (Mg) (*B1*). (Scale bars: 1 cm.) At higher magnification, strong hybridization signals were detected in the epithelial folds of the labial palps (Lp) but not in the vesicular connective tissue (Ct) (*B3*). Similar hybridization signals were seen in the digestive gland tubules (Dgt) (*B5*). Control sections with the sense riboprobe were devoid of labeling (*B2*, *B4*, and *B6*). (Scale bars: 80 μ m.)

in tissues from unchallenged (control) and challenged (24 h) oysters. In unchallenged oysters, strong hybridization signals were seen in epithelia of almost all tissues, namely gills, mantle, labial palps, stomach, digestive gland diverticula, intestine, and reproductive follicles in gonads (Fig. 5B). Very similar hybridization pictures were obtained with oysters observed 24 h after challenge (data not shown), which indicated that *Cg-bpi* is constitutively expressed in oyster epithelia. Moreover, numerous *Cg-bpi*-positive hemocytes were evidenced infiltrating the connective tissues of the different organs from challenged oysters (data not shown). No hybridization signal was observed with the *Cg-bpi* sense probe (Fig. 5B), revealing that the detection of *Cg-bpi* transcripts with the antisense riboprobe was specific.

Discussion

We have identified and characterized for the first time in an invertebrate, the oyster *C. gigas*, a BPI protein that we named *Cg-BPI*. It has significant similarities with two structurally related

proteins from mammals, namely LBPs and BPIs. Such proteins have also been identified in nonmammalian vertebrates (14–16) as well as in invertebrates (17, 18). However, the functional attributes of these homologues have not yet been defined with respect to LBP versus BPI activity. In the oyster *C. gigas* we have addressed this question by studying the biological activity of the protein and analyzing the gene expression in response to bacterial challenge.

The analysis of *Cg-BPI* amino acid sequence, including structural modeling and study of the predicted electrostatic surface potential (data not shown), revealed that the oyster protein contains the two characteristic conserved domains of BPI and related proteins from the family such as LBP, phospholipid transfer protein, and cholestryler ester transfer protein. Like hBPI, *Cg-BPI* is predicted to possess a boomerang shape with two barrels located at the N and C termini, connected by a central β -sheet (20). The N-terminal domain contains functional regions proposed to be involved in (i) LPS binding in hLBP and hBPI and (ii) LPS neutralization and bactericidal activity in BPI (21–23). The functional region II of hBPI contains five lysines that may engage in electrostatic interactions with the negatively charged groups of LPS (17, 23). Three lysines are conserved (at positions 119, 122, and 126 in hBPI precursor protein) in both hLBP and *Cg-BPI*. In LBP, two of these lysines were experimentally shown to mediate LPS binding (23). Synthetic peptides based on region II of hBPI possess antibacterial activity (20, 24). In addition, the *Cg-BPI* N-terminal domain was shown to contain the two conserved cysteines common to the lipid-binding family and involved in the formation of a disulfide bond (25) that is important for the function of rhBPI (26).

Whereas BPI and LBP present overall sequence similarity, they differ considerably in their predicted pI and net charge. Such differences might account for functional differences in antibacterial activity between BPI and LBP (27). *Cg-BPI* displays a theoretical pI of 9.3, which is close to the value for hBPI (9.4), whereas hLBP has a theoretical pI of 6.25. This suggests that the sequence identified may function as a BPI rather than LBP protein.

To ascertain this function, *Cg-BPI* was produced in *P. pastoris* as a recombinant protein (rCg-BPI) and studied for its LPS-binding, membrane-permeabilizing, and antibacterial activities. The interaction of rCg-BPI with LPS was shown by surface plasmon resonance analysis. The affinity constant obtained for rCg-BPI for LPS from *E. coli* (3.1×10^{-8} M) is in agreement with values obtained with known LBPs, such as the *Limulus* factor C, LBP, BPI, or polymyxin B, which range from 3.3×10^{-7} M to 2.3×10^{-10} M (28). The affinity of rCg-BPI for LPS indicates that *Cg-BPI* may bind to Gram-negative bacteria. This is supported by a bactericidal activity against *E. coli* SBS363. Interestingly, the activity observed against this strain, which harbors a LPS with short polysaccharide chain, was not observed against *E. coli* ML35, which harbors a LPS with a smooth/long polysaccharide chain. This is consistent with the more potent activity of hBPI against bacteria with short-chain LPS due to greater accessibility to lipid A (29, 30). Finally, similar to hBPI, which is bactericidal (31) and displays a permeabilizing effect on bacterial membranes (10), rCg-BPI induced permeabilization of the cytoplasmic membrane of *E. coli*. Altogether, the LPS-binding, the antibacterial, and the membrane-permeabilizing activity of rCg-BPI demonstrate that it is an invertebrate BPI that contributes to antibacterial defense.

Besides structural and biological properties, *Cg-BPI* appears to be similar to hBPI with respect to the localization of gene expression and to the expression profile in response to bacterial challenge. Originally, hBPI has been shown to be expressed in neutrophils (8), which are mobilized during an acute response to tissue sites of bacterial invasion (32). However, further studies have shown that hBPI is expressed in various mucosal epithelia where it can be up-regulated in response to aspirin-triggered antiinflammatory lipids (lipoxins) (33). Recently, an orthologous BPI protein has been characterized in mouse neutrophils. Constitutively expressed in lymphatic organs and tissues, the mouse *bpi* gene is strongly

inducible in various organs upon LPS stimulation (34). In *C. gigas* hemocytes, the *Cg-bpi* gene was expressed at low basal levels in unchallenged oysters, and its transcription appeared up-regulated in response to bacterial challenge to reach a maximum at 24 h. In addition, the challenge induced an increase in the number of *Cg-bpi*-expressing hemocytes. These were found both in blood circulation and as infiltrating the oyster connective tissues, which reveals a systemic reaction. This strongly suggests that LPS recognition may induce in oysters not only the transcription of *Cg-bpi* gene but also a process of hemocyte proliferation as observed in shrimp in response to a *Vibrio* infection (35). Interestingly, we showed that the *Cg-bpi* gene is also expressed in the epithelia of various organs of the oysters, namely gills, mantle, labial palps, and epithelia of the digestive system such as the stomach, digestive gland diverticula, and intestine. *Cg-bpi* transcripts have also been detected in follicles of the gonad. Whereas the expression of *Cg-bpi* is up-regulated in the hemocytes, it appears to be constitutive in the epithelia.

Epithelia represent one of the first barriers for protection against environmental microbes. In vertebrates, antimicrobial proteins and peptides have been identified as products of epithelial cells (36). In invertebrates, antimicrobial peptides are also known to be expressed in various epithelia. In *Drosophila melanogaster*, the expression of genes encoding antimicrobial peptides is induced in the epithelia of the respiratory tract, the oral region, the digestive tract, the malpighian tubules, and the male and female reproductive tracts (37). Interestingly, a defensin named *Cg-Def* has been characterized from the mantle of the oyster *C. gigas* (38) where it may colocalize with Cg-BPI. The oyster, which is continuously exposed to an environment rich in microorganisms, may have developed an efficient system to limit bacterial invasion. Through the constitutive expression of both defensin and BPI in epithelia, the bacterial populations may be under control and equilibrium may be reached between the immune system and the natural microflora of the oysters. Synergy between Cg-BPI and other oyster antimicrobials may actually occur as demonstrated between BPI and antimicrobial peptides such as defensins and cathelicidins from rabbit granulocytes in killing Gram-negative bacteria (39). Additionally, hemocytes are likely to contribute to an acute phase reaction upon microbial invasion by the transient expression of Cg-BPI and other antimicrobial effectors.

From the results presented with the identification of a BPI-related gene in the *C. gigas* oyster, this bivalve mollusk appears as an interesting model for studying the interaction between the host immune system and bacterial populations. In particular, it is attractive to determine how the oyster immune system communicates with commensal microflora and how it discriminates commensals from potentially harmful bacteria. From an evolutionary perspective, it will be of a great interest to further compare the biological properties of the mollusk Cg-BPI protein with its orthologous hBPI protein considering the natural flora encountered in these organisms.

Materials and Methods

Animals, Tissue Collection, and Immune Challenge. Adult *C. gigas* were purchased from a local oyster farm in Palavas (Gulf of Lion, France) and kept in sea water at 15°C. Oysters were challenged by adding heat-killed bacteria *Micrococcus luteus*, *Vibrio splendidus*, and *Vibrio anguillarum* (5×10^8 bacteria per liter) in sea-water tanks. Hemolymph was collected at different times (0, 15, 24, and 48 h) in antiaggregant modified Alsever solution (40). Hemocytes were collected by centrifugation ($700 \times g$, 10 min, 4°C). After hemolymph collection, oyster tissues were harvested by dissection.

Screening of a *C. gigas* Hemocyte cDNA Library and Northern Blot Analysis. A total of 36,864 clones from a oyster hemocyte cDNA library (19) were spotted onto high-density membranes, corresponding to 18,432 unique cDNAs. The EcoRI/XbaI fragment

from a cDNA clone (GenBank accession no. BQ427321) was radiolabeled as described previously (19) for high-density membrane screening. Positive clones were recovered from the cDNA library for subsequent sequencing. Transcript size was determined by Northern blot using the same probe, as previously described (19).

Sequence Analysis and Structure Modeling. Homology searches were performed with BLAST software (www.ncbi.nlm.nih.gov/blast). Deduced amino acid sequences were aligned by using ClustalW (<http://npsa-pbil.ibcp.fr>). Domain and signal peptide prediction was performed with the SMART (<http://smart.embl-heidelberg.de>) (41) and SignalP (www.cbs.dtu.dk/services/SignalP) software, respectively. Cg-BPI three-dimensional structure was predicted by using the hBPI crystal structure (Protein Data Bank ID code 1EWF) as a template (<http://bioserv.cbs.cnrs.fr>). The Protein Data Bank file of electrostatic surface potential was estimated by using the Swiss PDB Viewer, version 3.7 (42).

Quantitative *In Situ* Hybridization. The cDNA clone (GenBank accession no. BQ427321) was used as a template for the riboprobe preparation. [³⁵S]UTP-labeled antisense and sense riboprobes were generated from linearized cDNA plasmids by *in vitro* transcription using an RNA transcription kit, T₃ RNA polymerase (Roche, Meylan, France), and [³⁵S]UTP (Amersham, Saclay, France). After hybridization, by contact with the autoradiographic emulsion, the emissions from the [³⁵S]-riboprobe produce silver grains, the number of which is proportional to the hybridization signal.

Preparation of *C. gigas* tissues (serial sections) and hemocytes from a pool of five oysters, as well as *in situ* hybridization analyses, were performed as described (43) except for probe quantification. Briefly, hybridization signals were visualized after a 36-h (hemocytes) or 72-h (tissues) exposure. Control consisted in replacing the antisense riboprobe with the sense riboprobe. Specific labeling values (quantification of silver grain in cellular area) were determined by subtracting those obtained for sense probe from the total labeling values observed. For hemocytes, we quantified the silver grains using the software Image J applied with a minimal size of particles fixed at eight pixels. Quantification was expressed as AU corresponding to the total area of pixels into hemocytes. Data were analyzed by one-way analysis of variance using STATISTICA software (Statsoft, Maisons-Alfort, France). $P < 0.05$ was considered significant. The percentage of positive hemocytes was determined over 100 counted cells in triplicate per condition.

Production and Purification of Recombinant Cg-BPI (rCg-BPI). *Cg-bpi* cDNA was amplified by PCR using Isis DNA polymerase (Qiobiogene, Strasbourg, France) with the 5'-AAGACCCCGGCTT-ACAGACTAGAACATC-3' and 5'-AATTATTGCAGGCCGCGT-CTCAGCCACTGTATTTCAG-3' specific primers and further cloned into the SnaBI/NotI sites of the pPIC9K *Pichia* expression vector (Invitrogen, Carlsbad, CA). Five micrograms of the purified recombinant plasmid was linearized by SacI and transformed into *P. pastoris* by electroporation as recommended by the manufacturer (Invitrogen). Positive *P. pastoris* transformants were selected on yeast peptone dextrose plates supplemented with G418-sulfate at final concentrations of 0, 0.25, 0.75, 1, 1.5, and 2 mg/ml as recommended by the manufacturer (Invitrogen).

The production of rCg-BPI was performed in buffered methanol complex medium (1% yeast extract/2% peptone/100 mM potassium phosphate/1.34% yeast nitrogen base/4 × 10⁻⁴ g/liter biotin/0.5% methanol, pH 6.0). Methanol was added every 24 h to a final concentration of 0.5%. After a 3-day induction, the culture supernatant was precipitated successively with 20% and 50% ammonium sulfate. The 50% precipitate was solubilized in a 10 mM potassium phosphate buffer at pH 6.0 and dialyzed against the same buffer by using a Cellu-Sep dialysis tube (cutoff 6–8 kDa). The retentate was then loaded onto CM macroprep cation-exchange resin (Bio-Rad) equilibrated in 10 mM sodium phosphate buffer at pH 7.4. After

washing with equilibration buffer, rCg-BPI was eluted with 200 mM NaCl in equilibration buffer and quantified by using MicroBCA (Pierce, Rockford, IL). After purification, the production yield for rCg-BPI was estimated at 2 mg/liter of culture medium.

For use as positive control in our experiments, rhBPI₂₁, a recombinant N-terminal fragment of hBPI, was provided by XOMA (Berkeley, CA).

Identification of rCg-BPI. rCg-BPI excised from a 12% SDS polyacrylamide gel was reduced with an excess of DTT, alkylated with iodoacetamide, and hydrolyzed with trypsin (sequencing grade; Roche Molecular Biochemicals) at a proportion of 12.5 ng/ μ l enzyme. The resulting peptides were extracted from the gel, desalting, and concentrated on a C₁₈ ZipTip according to the manufacturer's recommendations (P10; Millipore). The eluted peptide mixture was used for MALDI TOF/TOF-MS, electrospray ionization MS, and electrospray ionization tandem MS analyses. Protein identification was performed by subjecting the *m/z* values to Mascot software at an adjusted peptide mass tolerance of \pm 100 ppm and/or 0.1 Da and at a fragment mass tolerance of \pm 0.5 Da.

Biological Activity. Bacterial strains. Bacterial strains were *E. coli* ML35 (smooth LPS) carrying the pBR322 plasmid (44) (generous gift of R. Lehrer, University of California, Los Angeles, CA), which is constitutive for cytoplasmic β -galactosidase, lacks lactose permease, and expresses a plasmid-encoded periplasmic β -lactamase, and *E. coli* SBS363, a Trp⁺ galU129 (truncated LPS) derivative of *E. coli* K12 strain D22 (generous gift of P. L. Boquet, Commissariat à l'Énergie Atomique, Saclay, France).

Antibacterial assays. Minimal inhibitory concentrations were determined at 30°C in poor broth medium (1% bactotryptone/0.5% NaCl, pH 7.5) as described in ref. 45 by serial dilutions of rCg-BPI and rhBPI₂₁ (0.02–10 μ M final concentration). For bactericidal assays, rCg-BPI and rhBPI₂₁ (0.25–5 μ M) were incubated with *E. coli* SBS363 (5×10^4 cfu/ml) in sodium phosphate buffer (pH 7.4) containing 200 mM NaCl. Colony-forming units (cfu) were counted by plating 10 μ l of the bacterial suspension on LB agar plates after 0, 1, and 3 h of incubation at 37°C.

1. Alexander C, Rietschel ET (2001) *J Endotoxin Res* 7:167–202.
2. Kim YS, Ryu JH, Han SJ, Choi KH, Nam KB, Jang IH, Lemaitre B, Brey PT, Lee WJ (2000) *J Biol Chem* 275:32721–32727.
3. Lee SY, Wang R, Söderhäll K (2000) *J Biol Chem* 275:1337–1343.
4. Roux MM, Pain A, Klimpel KR, Dhar AK (2002) *J Virol* 76:7140–7149.
5. Beschin A, Bilej M, Hanssens F, Raymakers J, Van Dyck E, Revets H, Brys L, Gomez J, De Baetselier P, Timmermans M (1998) *J Biol Chem* 273:24948–24954.
6. Koizumi N, Morozumi A, Imamura M, Tanaka E, Iwahana H, Sato R (1997) *Eur J Biochem* 248:217–224.
7. Thomas CJ, Kapoor M, Sharma S, Bausinger H, Zylian U, Lipsker D, Hanau D, Surolia A (2002) *FEBS Lett* 531:184–188.
8. Elsbach P, Weiss J (1993) *Immunobiology* 187:417–429.
9. Levy O (2004) *J Leukocyte Biol* 76:909–925.
10. Ooi CE, Weiss J, Elsbach P, Frangione B, Mannion B (1987) *J Biol Chem* 262:14891–14894.
11. Iovine NM, Elsbach P, Weiss J (1997) *Proc Natl Acad Sci USA* 94:10973–10978.
12. Weiss J (2003) *Biochem Soc Trans* 31:785–790.
13. Hamann L, Alexander C, Stamme C, Zahringer U, Schumann RR (2005) *Infect Immun* 73:193–200.
14. Kono T, Sakai M (2003) *Mol Immunol* 40:269–278.
15. Inagawa H, Honda T, Kohchi C, Nishizawa T, Yoshiura Y, Nakanishi T, Yokomizo Y, Soma G (2002) *J Immunol* 168:5638–5644.
16. Stenvik J, Solstad T, Strand C, Leiros I, Jorgensen TT (2004) *Dev Comp Immunol* 28:307–323.
17. Beamer LJ, Fischer D, Eisenberg D (1998) *Protein Sci* 7:1643–1646.
18. Mitta G, Galinier R, Tisseyre P, Allienne JF, Girerd-Chambaz Y, Guillouf F, Bouchut A, Coustau C (2005) *Dev Comp Immunol* 29:393–407.
19. Gueguen Y, Cadoret JP, Flament D, Barreau-Roumiguere C, Girardot AL, Garnier J, Hoareau A, Bachère E, Escoubas JM (2003) *Gene* 316:139–145.
20. Beamer LJ, Carroll SF, Eisenberg D (1997) *Science* 276:1861–1864.
21. Little RG, Kelner DN, Lim E, Burke DJ, Conlon PJ (1994) *J Biol Chem* 269:1865–1872.
22. Capodici C, Weiss J (1996) *J Immunol* 156:4789–4796.
23. Lampert N, Hoess A, Yu B, Park TC, Kirschning CJ, Pfeil D, Reuter D, Wright SD, Herrmann F, Schumann RR (1996) *J Immunol* 157:4648–4656.
24. Gray BH, Haseman JR (1994) *Infect Immun* 62:2732–2739.
25. Gray PW, Flagg G, Leong SR, Gumina RJ, Weiss J, Ooi CE, Elsbach P (1989) *J Biol Chem* 264:9505–9509.
26. Horwitz AH, Leigh SD, Abrahamson S, Gazzano-Santoro H, Liu PS, Williams RE, Carroll SF, Theofan G (1996) *Protein Expression Purif* 8:28–40.
27. Beamer LJ, Carroll SF, Eisenberg D (1998) *Protein Sci* 7:906–914.
28. Tan NS, Ng ML, Yau YH, Chong PK, Ho B, Ding JL (2000) *FASEB J* 14:1801–1813.
29. Weiss J, Beckerlite-Quagliata S, Elsbach P (1980) *J Clin Invest* 65:619–628.
30. Capodici C, Chen S, Sidorsky Z, Elsbach P, Weiss J (1994) *Infect Immun* 62:259–265.
31. Weiss J, Elsbach P, Olsson I, Odeberg H (1978) *J Biol Chem* 253:2664–2672.
32. Fierer J, Swancutt MA, Heumann D, Golenbock D (2002) *J Immunol* 168:6396–6403.
33. Levy O, Canny G, Serhan CN, Colgan SP (2003) *Biochem Soc Trans* 31:795–800.
34. Eckert M, Wittmann I, Rollinghoff M, Gessner A, Schnare M (2006) *J Immunol* 176:522–528.
35. Munoz M, Vandenbulcke F, Garnier J, Gueguen Y, Bulet P, Saulnier D, Bachère E (2004) *Cell Mol Life Sci* 61:961–972.
36. Ganz T (2002) *Proc Natl Acad Sci USA* 99:3357–3358.
37. Tzou P, Ohresser S, Ferrandon D, Capovilla M, Reichhart JM, Lemaitre B, Hoffmann JA, Imler JL (2000) *Immunity* 13:737–748.
38. Gueguen Y, Herpin A, Aumelas A, Garnier J, Fievet J, Escoubas JM, Bulet P, Gonzalez M, Lelong C, Favrel P, Bachère E (2006) *J Biol Chem* 281:313–323.
39. Levy O, Ooi CE, Weiss J, Lehrer RI, Elsbach P (1994) *J Clin Invest* 94:672–682.
40. Bachère E, Chagot D, Grizel H (1988) *Dev Comp Immunol* 12:549–559.
41. Schultz J, Milpitz F, Bork P, Ponting CP (1998) *Proc Natl Acad Sci USA* 95:5857–5864.
42. Guex N, Peitsch MC (1997) *Electrophoresis* 18:2714–2723.
43. Munoz M, Vandenbulcke F, Saulnier D, Bachère E (2002) *Eur J Biochem* 269:2678–2689.
44. Lehrer RI, Barton A, Ganz T (1988) *J Immunol Methods* 108:153–158.
45. Destoumieux D, Bulet P, Strub J-M, Bachère E (1999) *Eur J Biochem* 266:335–346.
46. Ferguson AD, Welte W, Hofmann E, Lindner B, Holst O, Coulton JW, Diederichs K (2000) *Structure (London)* 8:585–592.

Assays for bacterial membrane permeability. The effect of rCg-BPI and rhBPI₂₁ on integrity of the bacterial membranes was assessed by spectrophotometric assays as described in ref. 44 using *E. coli* ML-35 pBR322. Briefly, bacteria at OD₆₀₀ = 0.4–0.6 were washed in 10 mM sodium phosphate buffer (pH 7.4), resuspended in this buffer to \approx 5 \times 10⁷ cfu/ml (OD₆₀₀ = 0.2), and kept on ice until used. ONPG (Sigma) was used as chromogenic substrate for β -galactosidase. The bacterial cell suspension (50 μ l) was distributed in 96-well polystyrene microplates in a final volume of 100 μ l containing 2.5 mM ONPG and either rCg-BPI or rhBPI₂₁ (5 and 10 μ M). The incubation medium was 10 mM sodium phosphate buffer (pH 7.4). Control was the omission of recombinant protein. Microplates were incubated at 25°C for 30 min, and OD was monitored at 405 nm for ONPG hydrolysis by using a Multiscan EX microplate reader (Labsystems).

LPS-binding activity. Surface plasmon resonance experiments were carried out at 25°C using a BIACORE 3000 apparatus (Biacore, Uppsala, Sweden). rCg-BPI was immobilized onto a CM5 chip (Biacore) via primary amino groups according to the manufacturer's instructions. The running buffer was 10 mM Hepes (pH 7.4), 150 mM NaCl, and 3 mM EDTA. For binding experiments, purified diphosphoryl lipid A from *E. coli* F583 Rd mutant and LPS from *E. coli* O26:B6 (Sigma) were used. Lipids were sonicated (15 min, 25°C) and injected simultaneously at different concentrations into the measuring and control (no protein immobilized) flow cells at a high flow rate (50 μ l/min) to limit mass transport effect. Kinetic parameters were calculated by using a Langmuir 1:1 global fitting model from BIAevaluation 4.1 software (Biacore). Here the differential rate equation directly describes the experimental binding curves at several LPS and lipid A concentrations assuming that lipids were in a monomeric state.

We are grateful to Prof. J. Weiss (University of Iowa) and Dr. A. Givaudan (Université Montpellier 2) for helpful discussions as well as Prof. R. Lehrer and Dr. P. L. Boquet for providing the strains *E. coli* ML-35 and *E. coli* SBS363, respectively. We also thank M. Leroy for technical assistance. This work was supported by Ifremer, the Centre National de la Recherche Scientifique, and the University of Montpellier 2. It was also part of a collaborative International Cooperation for Development project supported by the European Community through Immunaqua Contract ICA4-CT-2001-10023.